Then we have

$$f(x)=\frac{8\pi cVm^3}{4\lambda h^3N\sin(\frac{1}{2}\varphi)}\int_{v=u}^{v=v_{\max}}vdv$$

$$=\frac{\pi cVm^3}{\lambda h^3N\sin(\frac{1}{2}\varphi)}(v_{\max}{}^2-u^2)$$

$$=\frac{\pi cVm^3}{\lambda h^3N\sin(\frac{1}{2}\varphi)}\left(v_{\max}{}^2-\frac{c^2}{4\lambda^2\sin^2(\frac{1}{2}\varphi)}x^2\right),$$

where the variable is the wavelength shift x. Knowing this relation we can determine the shape of the Compton band. For $x=0$ we have the peak of the parabola. The two ends are obtained by replacing x by $x_m=\pm(2\lambda/c)\sin(\frac{1}{2}\varphi)v_{\max}$. This result is valid for scattering angles larger than φ_0. For the case of $\varphi<\varphi_0$, the shaded part of Fig. 1 is divided in two parts lying on either side of the plane AB (Fig. 11). The part to the right of this plane gives a section of the parabola mentioned above, while the other part to the left of the plane AB gives a linear section of the profile. Using for the variable x the limits

$$(2\lambda/c)\sin(\tfrac{1}{2}\varphi)(-\tfrac{1}{2}s)\leqslant x\leqslant(2\lambda/c)\sin(\tfrac{1}{2}\varphi)(v_{\max}-s),$$

we find easily

$$f(x)=\frac{\pi cVm^3}{\lambda h^3N\sin(\frac{1}{2}\varphi)}\left(s^2+\frac{sc}{\lambda\sin(\frac{1}{2}\varphi)}x\right),$$

which represent a straight line. On the basis of this calculation we plotted the curve of Fig. 3 for $\varphi=10°$.

ACKNOWLEDGMENTS

We are greatly indebted to Professor K. Alexopoulos for many stimulating discussions during this work and also for his comments on the manuscript. We express also our gratitude to Dr. C. A. Beevers of Edinburgh University, who drew the curve of Fig. 10 according to his method.

PHYSICAL REVIEW VOLUME 145, NUMBER 2 13 MAY 1966

Energy and Atomic Configuration of Complete and Dissociated Dislocations. I. Edge Dislocation in an fcc Metal*

R. M. J. Cotterill and M. Doyama
Argonne National Laboratory, Argonne, Illinois

(Received 18 September 1964; revised manuscript received 20 December 1965)

The arrangement of atoms around an edge dislocation in copper has been calculated by a variational method using a central-force approximation. The pairwise interaction between discrete atoms was represented by a Morse potential function. In the calculation of the complete dislocation, the atoms were not permitted to relax in a direction parallel to the dislocation line. This prevented dissociation. Linear-elasticity theory is found to break down inside a core radius of 9 Å for a complete ⟨112⟩ dislocation [Burgers vector $=(a_0/2)\langle 110\rangle$, where a_0 is the lattice constant]. The corresponding core energy is 0.65 eV per {112} plane. If the core is replaced by a cylindrical hole of radius r_{eh} (the *equivalent hole* radius), the inside of which is hollow and outside of which linear-elastic theory holds at all points, this radius is 0.8 Å. The complete dislocation was found to have a width of 13 Å (i.e., about five Burgers vectors). The core region is found to be neither hollow nor like a liquid. If the atoms are permitted to relax in a direction parallel to the dislocation line, the dislocation spontaneously dissociates into two Heidenreich-Shockley partials; and this process involves no activation energy. A stacking fault of infinite extent has an energy of 30 erg cm^{-2} for the potential and truncation used in the calculation. Certain precautions must be taken to ensure that the separation distance of the partials is the same as the distance given by elastic theory. Several different potential forms were used in the calculations of stacking-fault energy. The stacking-fault energy is found to be critically dependent upon the form of the interatomic potential. For the pseudopotential for aluminum given by Harrison, the stacking-fault energy is approximately 250 erg cm^{-2}.

I. INTRODUCTION

THE elastic-continuum treatment of dislocations in metal crystals has always suffered from difficulties associated with the dislocation core. Expressions for the stresses around a dislocation, derived by the continuum method, invariably have a singularity at the center of the dislocation. It is clear that such a singularity does not occur in a real crystal. This difficulty is usually overcome by treating separately that part of the crystal which lies inside a small cylinderical core whose axis is the dislocation and the radius of which is r_c, say. This part is referred to as the dislocation core, and the linear elastic theory is said to break down in this region. The integrations which are involved in calculations of dislocation energy use r_c as a lower limit of

* Based on work performed under the auspices of the U. S. Atomic Energy Commission.

the radius. This procedure is unsatisfactory in that without knowing the exact arrangements of atoms in the core one has difficulty in choosing a value of r_c. Moreover, even when r_c has been chosen, there is no satisfactory way of dealing with that part of the crystal which lies inside this radius. This paper describes a method by which these difficulties can be resolved. It involves a three-dimensional atomistic treatment in which the atoms interact with one another with forces which are purely central.

A rough estimate of the core energy has been made by Bragg,[1] who obtained a value of 1 eV per atom plane using the fact that the energy density in the core cannot exceed the latent heat of melting. Hasiguti and Doyama[2] arrived at a value of 1.1 eV per atom plane in a calculation involving two dislocations of opposite sign separated by one atomic plane This configuration is equivalent to a row of vacancies. Cottrell[3] assumed that Hooke's law holds inside the core and found a core energy of 1.3 eV per atom plane. Huntington,[4] who calculated the electrostatic energy between atoms in a dislocation in rocksalt, obtained approximately 0.5 eV per atom plane for an edge dislocation in that material. This appears to have been the first calculation of this type to be based on a discrete atom model. Huntington *et al.*[5] refined these calculations for both edge and screw dislocations in the same material. Englert and Tompa[6] have used a two-dimensional model to calculate the positions of atoms in a plane normal to a ⟨110⟩ dislocation in argon.

In recent years calculations of the energies and atomic configurations of clusters of point defects have been greatly facilitated by application of computer techniques and the use of discrete-atom models. The interactions between the atoms in a metal crystal have usually been represented by a Born-Mayer potential[7] or a Morse potential.[8] The considerable success of these calculations has been summarized by Damask and Dienes.[9] This paper reports the results of a project which extends the method to the case of the edge dislocation in a three-dimensional copper crystal. The calculations involved the use of a Morse potential and were carried out with the aid of a CDC 3600 digital computer. The use of a Morse crystal (with its inherent stability) rather than a Born-Mayer crystal (whose stability can only be achieved by application of an external force) is discussed later in the paper.

Heidenreich and Shockley[10] have shown that it is energetically favorable for a complete dislocation in a face-centered lattice to split into two partial dislocations, the region between the latter being a stacking fault. In the present study both the complete and the dissociated configurations were examined. Because calculations which are based on the elastic-continuum theory do not hold for the core region, it is not possible within the framework of this theory to treat dissociated dislocations in which the separation distance of the partials is of core dimensions. It is not known, therefore, whether or not there is an activation energy for dissociation. As is shown later, the use of an atomistic model permits clarification of this point.

If one is to put any reliance on the results for the dissociated dislocation, one would have to be sure that the method of calculation is capable of giving an acceptable value of the stacking-fault energy. This value would be obtained from a calculation involving a fault of infinite extent (i.e., a case where the effects of the partial dislocations can be ignored). Calculations of the stacking-fault energy γ in fcc metals, based on the electron theory of metals, have been published.[11,12] The essentials of these treatments are as follows. Electrons in closed shells make only a small contribution to γ because they mostly affect the interactions between nearest neighbors, and nearest-neighbor relationships are not violated at a stacking fault. The contribution of the conduction electrons to γ arises from the change in the shape of the Fermi surface near the Brillouin-zone boundaries. Because of this, multivalent metals such as aluminum should have a high γ, because the conduction electrons overlap the boundaries of the first zone; and a stacking fault then produces a considerable change in energy. Metals such as copper, silver, and gold, on the other hand, have a low γ. These metals have nearly spherical Fermi surfaces which barely touch the zone boundary.[13] In the present paper, a quite different approach is taken. The stacking-fault energy is calculated by taking into account the pairwise interaction between atoms and assuming central forces.

The calculations described in this paper involved the use of a Morse potential function and also several more complex functions. These functions and their application to calculations on lattice defects are discussed in Sec. II. The calculations on stacking faults, complete edge dislocations, and dissociated edge dislocations are described in Secs. III, IV, and V, respectively.

---

[1] W. L. Bragg, *Symposium on Internal Stress* (Institute of Metals, London, 1947), p. 221.

[2] R. R. Hasiguti and M. Doyama, Bull. Japan Inst. Metals, October (1952) [in Japanese]; Bull. Phys. Soc. Japan, April (1953).

[3] A. H. Cottrell, *Dislocations and Plastic Flow in Crystals* (Clarendon Press, Oxford, England, 1956), p. 39.

[4] H. B. Huntington, Phys. Rev. **59**, 942A (1941).

[5] H. B. Huntington, J. E. Dickey, and R. Thomson, Phys. Rev. **100**, 1117 (1955).

[6] A. Englert and H. Tompa, J. Phys. Chem. Solids **21**, 306 (1961).

[7] M. Born and E. Mayer, Z. Physik **75**, 1 (1932).

[8] P. M. Morse, Phys. Rev. **34**, 57 (1929).

[9] A. C. Damask and G. J. Dienes, *Point Defects in Metals* (Gordon and Breach Science Publishers, Inc., New York, 1964), p. 11.

[10] R. D. Heidenreich and W. Shockley, *Report on Strength of Solids* (The Physical Society, London, 1948), p. 57.

[11] A. Seeger and H. Bross, Z. Physik **145**, 161 (1956).

[12] A. Seeger, *Defects in Crystalline Solids* (The Physical Society, London, 1955), p. 328.

[13] J. M. Ziman, *Principles of the Theory of Solids* (University Press, Cambridge, England, 1964).

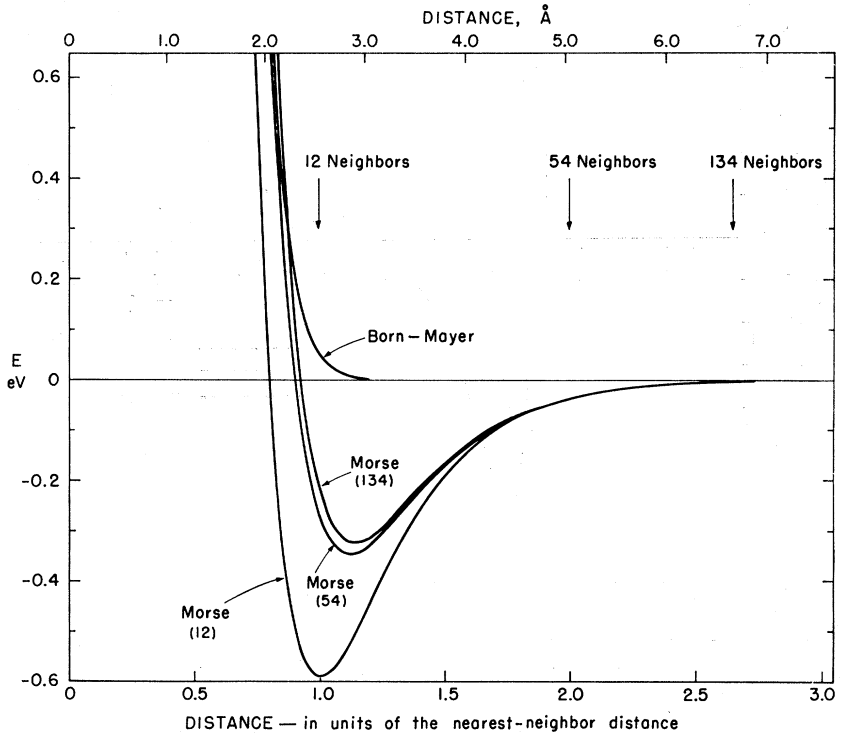

FIG. 1. Energy as a function of distance for the Born-Mayer potential and Morse potential in copper. Morse curves are plotted for three different truncations. The Morse curves for truncations at more than 134 atoms coincide with the curve for truncation at 134 atoms.

II. INTERATOMIC POTENTIAL FUNCTIONS

In the present calculations the interaction energy between atoms was represented by a central-force function. In most cases a Morse function was used. The interaction energy $E(r_{ij})$ of a pair of isolated atoms is then given by

$$E(r_{ij})=D\{\exp[-2\alpha(r_{ij}-r_0)] -2\exp[-\alpha(r_{ij}-r_0)]\}, \quad (1)$$

where r_{ij} is the distance between the two atoms, D is the dissociation energy of the pair, r_0 is the equilibrium separation distance of the two atoms, and α is a constant which is effectively a measure of the hardness" of the interaction. The energy of any atom in the crystal is then E_i, where

$$E_i=\sum_{j=1}^{j=J} E(r_{ij}), \quad (2)$$

and where J is the number of atoms in the sphere of influence. J is, of course, related by a geometrical factor to the distance over which the interaction extends. Girifalco and Wiezer[14] have derived constants for the Morse potential for several different metals. For copper these authors give $\alpha=1.3588$ Å^{-1}, $r_0=2.8660$ Å, and $D=0.34290$ eV.

The values of the constants must, of course, depend upon J. Clearly, if J were 12 (i.e., only nearest neighbors interact), then r_0 would be equal to the nearest-neighbor distance. The values given by Girifalco and Wiezer were obtained with a large crystal (containing 4000 atoms) in which each atom was allowed to interact with all other atoms. The field of each atom therefore virtually extended to infinity. In variational calculations of the type used here, the successive relaxations of atoms are rather time consuming even when the latest computers are employed; so it becomes impracticable to consider such long-range interactions. Moreover, one cannot be certain that the field of an atom is still adequately described by a Morse function at distances greater than a few nearest-neighbor distances. One would expect screening effects from other atoms to modify the field. For both of these reasons it becomes desirable to truncate the potential (i.e., to limit J to some convenient finite number). It can be shown[15] that as J decreases from infinity to 12 (the number of nearest-neighbor atoms in the perfect fcc lattice), the value of r_0 decreases from about $1.3d_0$ to d_0, where d_0 is the nearest-neighbor distance. There is also a corresponding variation in α and D. In the work described here the potential was truncated at 176 neighboring atoms and the constants were $r_0=2.9130$ Å, $a_0=3.6028$ Å, $D=0.3226$ eV, and $\alpha=1.2866$ Å^{-1}, where a_0 is the lattice constant ($=d_0\sqrt{2}$). These constants were determined by the method described by Girifalco and Wiezer.[14] This method uses the fact that bulk crystal

[14] L. A. Girifalco and V. G. Wiezer, Phys. Rev. **114**, 687 (1959).

[15] M. Doyama and R. M. J. Cotterill, Bull. Am. Phys. Soc. **10**, 323 (1965).

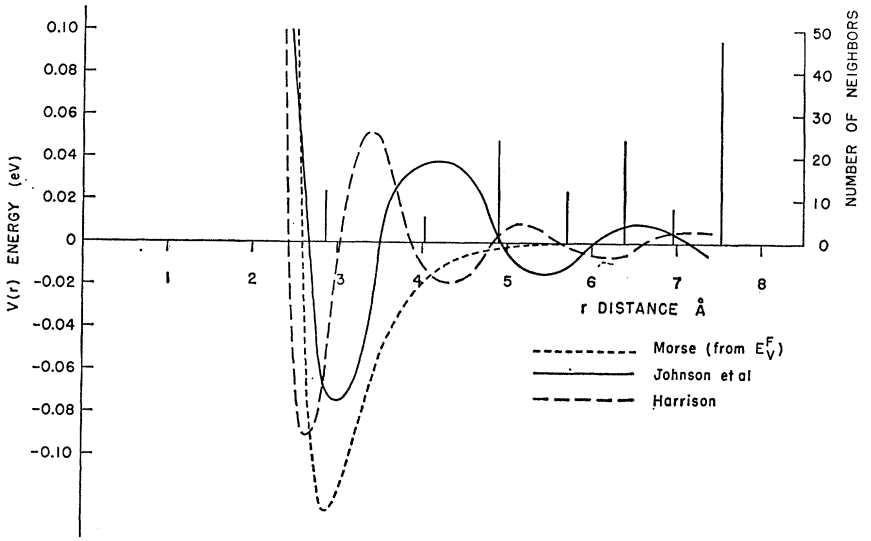

FIG. 2. Energy as a function of distance for various potentials in aluminum. The distribution of atoms in the first few neighboring atomic shells is also indicated.

properties calculated with a particular truncated potential must match the experimental values of those properties. In this case the properties chosen were the energy of sublimation, the bulk modulus, and the lattice constant. An additional constraint was that the Born stability criteria[16] have to be satisfied. Moreover, the potential used here gives values of the elastic constants which are in good agreement with the experimental values. The experimental values of C_{11}, C_{12}, and C_{44} are 17.88×10^{11}, 12.6×10^{11}, and 8.35×10^{11} dyn cm^{-2}, respectively.[17] The theoretical values derived with the Morse potential were 15.98×10^{11}, 11.22×10^{11}, and 11.22×10^{11} dyn cm^{-2} for the same quantities.

As was noted earlier, many previous atomistic calculations on lattice defects have involved the use of a Born-Mayer potential. In the present study a Morse potential function was preferred to a function of the Born-Mayer type for reasons which are best understood by reference to Fig. 1. In that figure both functions are plotted as a function of radial distance for copper. The Morse potential has both repulsive and attractive terms. The Born-Mayer potential has only a repulsive term, and a crystal which obeys this function must be artificially held together by forces applied to its surface.

One of the parameters which was calculated in the present study was the stacking-fault energy γ. It was decided that a calculation of γ for a whole series of different potential forms should be carried out. Interatomic potentials for aluminum have been published recently by Johnson *et al.*[18] and by Harrison.[19] The potential derived by Johnson *et al.* is for liquid aluminum at a temperature of 750°C. It was derived from neutron scattering data. The potential given by Harrison is for solid alumiun and was derived from pseudopotential theory. These two potentials are plotted, together with the Morse potential (176 neighbors) for aluminum,[20] in Fig. 2.

The next three sections of the paper describe in detail the calculations and results for stacking faults, complete edge dislocations, and dissociated edge dislocations, respectively.

III. CALCULATIONS OF STACKING-FAULT ENERGY

The calculations of γ were performed with a fault which was effectively infinite (as opposed to a fault bounded by partial dislocations). The upper part of the atomistic crystal, which was fed into the computer, was displaced by an amount $(a_0/6)\langle 112\rangle$ relative to the lower part, where a_0 is the lattice parameter. Only the intrinsic type of fault was examined, and in this particular study the atoms were not permitted to relax (as they were in the dislocation calculations described in the next section). Calculations on stacking faults involving relaxations of the atoms are now being carried out, but these will not be described here. The preliminary results of that study show that there is an expansion of the spacing between planes of about 1% near the fault.

Values of γ for copper were obtained with the Morse potential discussed in Sec. II and with the Born-Mayer potential given by Gibson *et al.*[21,22] and Johnson and

[16] M. Born, Proc. Cambridge Phil. Soc. **36**, 160 (1940).
[17] H. B. Huntington, *Solid State Physics*, edited by F. Seitz and D. Turnbull (Academic Press Inc., New York, 1958), Vol. 7, p. 213.
[18] M. D. Johnson, P. Hutchinson, and N. H. March, Proc. Roy. Soc. (London) **282A**, 283 (1964).
[19] W. A. Harrison, Phys. Rev. **129**, 2512 (1963).
[20] R. M. J. Cotterill and M. Doyama, Bull. Am. Phys. Soc. **10**, 1095 (1965). Further details to be published.
[21] G. H. Vineyard and J. B. Gibson, Bull. Am. Phys. Soc. **6**, 158 (1961).
[22] J. B. Gibson, A. N. Goland, M. Milgram, and G. H. Vineyard, Phys. Rev. **120**, 1229 (1960).

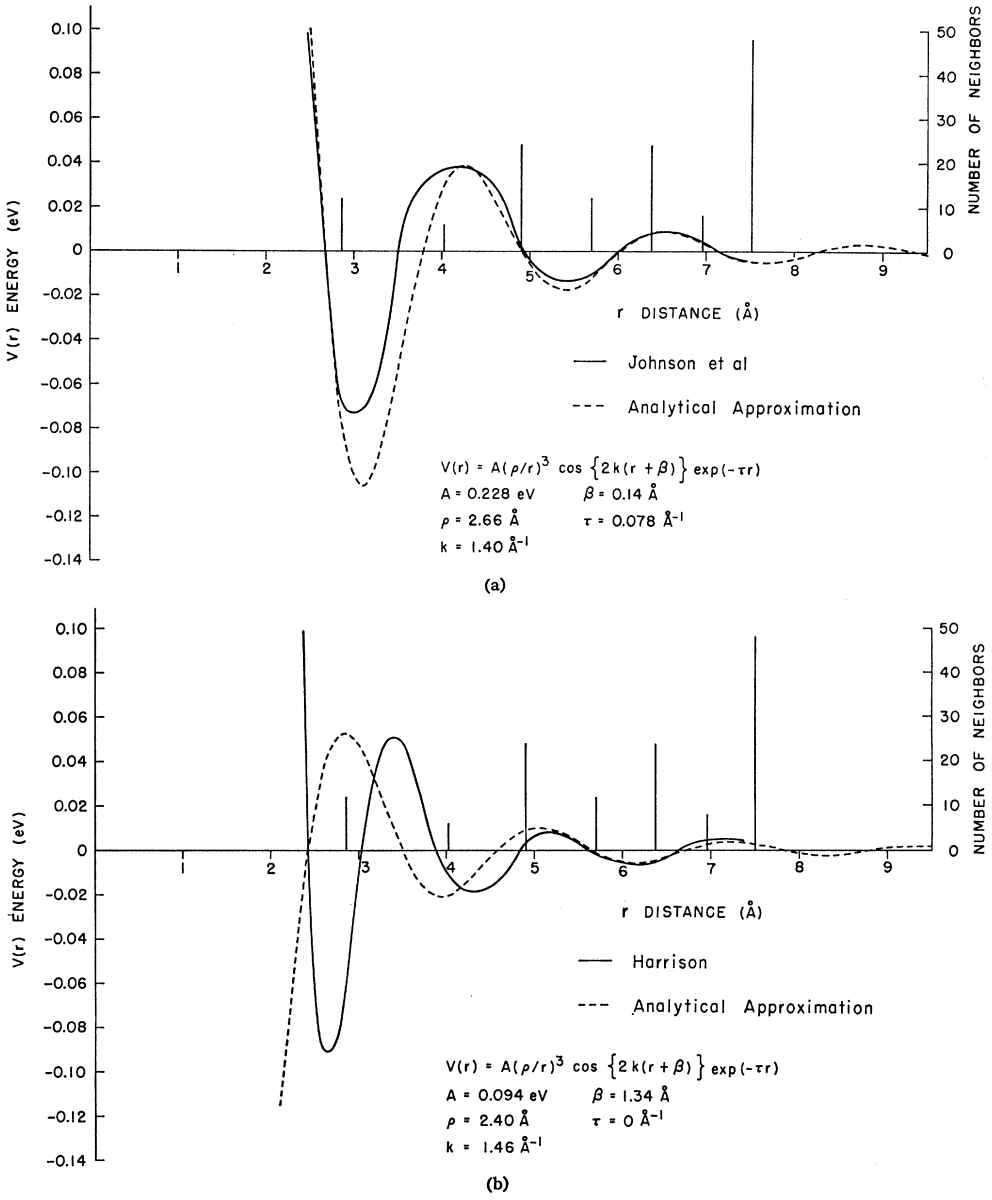

FIG. 3. (a) Comparison of the actual and analytical forms of the potential function derived by Johnson *et al.* (Ref. 18). The constants for the analytical form ($A=0.228$ eV, $\rho=2.66$ Å, $K=1.40$ Å^{-1}, $\beta=0.14$ Å, and $\tau=0.078$) were found to give a better fit than those given by Johnson *et al.* The analytical approximation gives a good fit beyond a distance of 6 Å. (b) Comparison of the actual and analytical forms of the potential function derived by Harrison (Ref. 19). The analytical approximation gives a good fit beyond a distance of 5.5 Å.

Brown[23] (see Fig. 1). Calculations of γ for aluminum were made for the Morse potential and for the potentials given by Johnson *et al.*[18] and by Harrison[19] (see Fig. 2). No Born-Mayer potential was available for aluminum. In the case of the calculation using the potentials of Johnson *et al.* and Harrison, values of γ were obtained for the actual potential derived from neutron scattering data both with and without the approximate analytical form for large radii suggested by Johnson *et al.* This analytical solution has the form

$$V(r)=A(\rho/r)^3\cos\{2K(r+\beta)\}\exp(-\tau r)\,. \quad (3)$$

For the Johnson *et al.* potential the constants are $A=0.228$ eV, $\rho=2.66$ Å, $K=1.40$ Å^{-1}, $\beta=0.14$ Å, and $\tau=0.078$ Å^{-1}. (These constants give a better fit than those given by Johnson *et al.*, viz., $A=0.041$ eV, $\rho=2.65$ Å, $K=1.37$ Å^{-1}, $\beta=1.95$ Å, and $\tau=0.18$ Å^{-1}.) The actual potential and the analytical solution are plotted in Fig. 3(a) for the sake of comparison. If the same analytical form is used for the Harrison potential, the constants are $A=0.094$ eV, $\rho=2.40$ Å, $K=1.46$ Å^{-1}, $\beta=1.34$ Å, and $\tau=0$. This analytical solution is plotted, together with the actual potential given by Harrison, in Fig. 3(b).

Various truncations were used in the calculations. For the nonanalytical forms of the Johnson *et al.* potential and the Harrison potential the truncation was determined by the extent of the curves published by

[23] R. A. Johnson and E. Brown, Phys. Rev. 127, 446 (1962).

these authors. In each case these oscillatory curves extend out to about 8 Å, and this corresponded to the inclusion of everything out to and including the seventh neighbor shell, a total of 134 neighboring atoms in all. Various truncations were used for the remaining forms, i.e., the Morse and Born-Mayer potentials. An effectively infinite truncation was used for the Johnson *et al.* potential and Harrison potential in which the analytical approximations were used beyond 7 Å, (using about 4000 neighbors). Morse potential calculations for aluminum were carried out using constants derived by two different methods. As has been pointed out elsewhere,[20,24] constants for the Morse potential derived from the experimental value of the sublimation energy E_S give anomalously high absolute values for the formation energy of point defects.[25] An alternative method for deriving the constants involves the use of the experimental value of the single vacancy formation energy, E_V^F. For both sets of constants, various truncations were used.

Table I shows the results for each of the sixteen different calculations of γ. To begin with, one may note that γ for copper calculated by using a Born-Mayer potential is vanishingly small. Experimental values of γ for copper lie in the range 30–80 erg cm^{-2}.[26–28] As might be expected from the shape of this potential (see Fig. 1), the result is not affected by tightening the truncation from 4000 atoms to 176 atoms. Even for the effectively infinite truncation the Morse potential gives a larger value of γ than does the Born-Mayer potential. The absolute value of γ is still quite low, however. It increases as the truncation is tightened, and for a truncation at 176 neighboring atoms the value is quite reasonable (30.8 erg cm^{-2}). It is for this reason that the 176 neighbor truncation was used in the calculations on dislocations described elsewhere in this paper.

Comparing the values of γ obtained for aluminum and copper by use of a Morse potential whose constants were derived through the relevant values of E_S, we find that for equivalent truncations the results are very similar. In fact, they differ by only a few percent. This is in disagreement with experiment. The value of γ in aluminum is generally regarded as being in the region of 200 erg cm^{-2} [12] (i.e., perhaps three to five times the value of γ for copper). It is not clear at this time just why the calculated values of γ for copper and aluminum should be so close to each other.

The Morse potential whose constants were calculated by using E_V^F instead of E_S gives very poor results. For all three truncations listed in the table the derived values of γ were very small and negative. The results in this case are not very dependent upon the truncation. This partly a reflection of the fact that the potential is in this case quite "narrow" compared with the potential derived from E_S. The constants of the potential also show no change with truncation in this range.

The results for the more complex potentials are on the whole more encouraging. It cannot be emphasized too strongly, however, that calculations with these potentials are at a very early stage of development. These preliminary results should not be taken too seriously. One difference between calculations with the complex potentials and those employing the simpler potentials concerns the effect of truncation. It can be seen from the table that the effect of truncation on calculations with the potentials of Johnson *et al.* and Harrison is to decrease γ. For a truncation at 4000 atoms the Johnson *et al.* potential gives $\gamma = 8.3$ erg cm^{-2}, whereas for a truncation at 134 atoms it gives $\gamma = -108$ erg cm^{-2}.[29] Comparing the two potential forms given by Johnson *et al.* and Harrison, respectively, for the same truncation (at 134 atoms), we find values of -108 and 91 erg cm^{-2}. It is not surprising that these potentials give values of γ which are approximately equal and opposite. Beyond the first shell of neighbors the potentials are almost exactly 180° out of phase with each other. For an effectively infinite truncation (4000 atoms) the Harrison potential gives $\gamma = 253.2$ erg cm^{-2}, which is in good agreement with the generally accepted value of 200 erg cm^{-2} for aluminum.[12]

Further calculations of γ using the more complex potentials are required. One urgent need is for pseudopotential curves for copper corresponding to the curve for aluminum given by Harrison. One hopes that such curves would produce relative values of γ for aluminum and copper which are in better agreement with experiment. It would be desirable, too, to have pseudopotential curves which extend out to radii considerably greater than the present limits of about 8 Å, because one can never be sure just how badly the results are affected by truncation. It is too early to say whether or not simple pairwise calculations in the central force approximation will ever be capable of giving acceptable

[24] Details are given in the two review papers by R. M. J. Cotterill and M. Doyama in *Lattice Defects and Their Interactions*, edited by R. R. Hasiguti (Gordon and Breach, Science Publishers, Inc., New York, 1966).

[25] When Morse potentials are used to calculate the formation energy of point defects, the absolute values of the latter are always rather high. Electron redistribution around the defect must account for part of the discrepancy. Another source of error may arise from the fact that the method used in deriving the constants of the Morse potential implicitly assumes that the electron environment which prevails during the measurement of the sublimation energy is the same as that prevailing during the measurement of the elastic constants. This is probably not true because the evaporation of a neutral atom from the surface requires first the localization of an electron at the atom which is to be removed. Because of these difficulties, an alternative approach may be used which links the Morse potential to the experimental value of E_V^F, the vacancy formation energy, rather than E_S, the sublimation energy.

[26] A. Howie and P. R. Swann, Phil. Mag. **6**, 1215 (1961).

[27] L. M. Brown, Phil. Mag. **10**, 441 (1964). L. M. Brown and A. R. Thölén, Discussions Faraday Soc. **38**, 35 (1964).

[28] T. Jössang, M. J. Stowell, J. P. Hirth, and J. Lothe, Acta Met. **13**, 279 (1965).

[29] This large negative value of γ is a direct result of truncation. Its appearance should not be taken to indicate that the hcp phase is more stable than the fcc structure. This would necessarily be so only for a truncation at next-nearest neighbors.

TABLE I. Calculations of γ for various analytical and nonanalytical potentials.

Born-Mayer: $V(r)=L\exp(-\lambda r)$

Metal	Constants	Truncation	L(eV)	λ(Å^{-1})	γ erg cm^{-2}
Copper	Gibson *et al.*	4000 atoms	0.053	13.9	0.007
		176 atoms	0.053	13.9	0.007

Morse: $V(r)=D\{\exp(-2\alpha[r-r_0])-2\exp(-\alpha[r-r_0])\}$

Metal	Constants	Truncation	D(eV)	α(Å^{-1})	r_0(Å)	γ erg cm^{-2}
Copper	Derived from E_S	4000	0.3236	1.2941	2.9133	0.422
		200	0.3228	1.2888	2.9135	17.9
		176	0.3226	1.2866	2.9130	30.8
Aluminum	Derived from E_S	4000	0.2774	1.1180	3.3005	0.412
		200	0.2763	1.1119	3.3013	16.3
		176	0.2761	1.1096	3.3007	27.9
		134	0.2762	1.1039	3.2966	43.8
	Derived from $E_V{}^F$	4000	0.1262	2.2623	2.8823	−0.37
		176	0.1262	2.2623	2.8823	−0.37
		134	0.1262	2.2623	2.8823	−0.32

Jonson *et al.*: $V(r)=A(\rho/r)^3\cos\{2K(r+\beta)\}\exp(-\tau r)$

Metal	Constants	Truncation	A(eV)	ρ(Å)	K(Å^{-1})	β(Å)	τ(Å^{-1})	γ erg cm^{-2}
Aluminum	With analytical approximation at large radii	4000	0.228	2.66	1.40	0.14	0.078	8.3
	Nonanalytical	134						−108.0

Harrison: $V(r)=A(\rho/r)^3\cos\{2K(r+\beta)\}\exp(-\tau r)$

Metal	Constants	Truncation	A(eV)	ρ(Å)	K(Å^{-1})	β(Å)	τ(Å^{-1})	γ erg cm^{-2}
Aluminum	With analytical approximation at large radii	4000	0.094	2.40	1.46	1.34	0	253.2
	Nonanalytical	134						91.0

values of γ. If scattering of electrons or changes in electron density at the fault really are the predominating effects, such calculations may not be successful unless electron redistribution can be allowed for in the interatomic potential in a self-consistent manner.

The calculations described in the remainder of this paper involve only the Morse potential.

IV. CALCULATION OF THE ENERGY AND ATOMIC CONFIGURATION OF A COMPLETE EDGE DISLOCATION

A. Nature of the Problem

According to the linear isotropic elastic continuum theory, the displacements parallel to the three axes x, y, and z, due to an edge dislocation lying along the y axis, are respectively[30]

$$u=\frac{b}{2\pi}\left[\arctan\left(\frac{z}{x}\right)+\frac{1}{2(1-\nu)}\frac{xz}{r^2}\right],$$
$$v=0, \tag{4}$$
$$w=\frac{b}{4\pi(1-\nu)}\left[(2\nu-1)\ln r+\frac{x^2}{r^2}\right],$$

where b is the Burger's vector, ν is Poisson's ratio, and r is $(x^2+z^2)^{1/2}$. The elastic energy per unit length of the dislocation is, for a sufficiently large crystal,[30]

$$E^E=\frac{\mu b^2}{4\pi(1-\nu)}\left[\ln\left(\frac{r_1}{r_C{}^E}\right)-1\right]+E_{\text{core}}{}^E, \tag{5}$$

where μ is the shear modulus and r_1 is the outer radiius of the crystal containing the dislocations. The second term in the brackets arises from relaxation of surface stresses. The superscript letter E is used to denote applicability to the case of an edge dislocation. The energy per unit length of a cylinder of radius r, inside the crystal, having the dislocation located at its axis, is

$$E^E(r)=\frac{\mu b^2}{4\pi(1-\nu)}\left[\ln\left(\frac{r}{r_C{}^E}\right)\right]+E_{\text{core}}{}^E. \tag{6}$$

The difficulties associated with the choice of $r_C{}^E$ and $E_{\text{core}}{}^E$, the core energy, can best be appreciated by reference to Fig. 4, which is a plot of dE/dr against r. Differentiating Eq. (6) with respect to r, we have

$$dE^E/dr=\frac{\mu b^2}{4\pi(1-\nu)}\frac{1}{r}. \tag{7}$$

The quantity dE^E/dr, which is plotted as the dashed

[30] J. Friedel, *Dislocations* (Addison-Wesley Publishing Company, Inc., Reading, Massachusetts, 1963), p. 20.

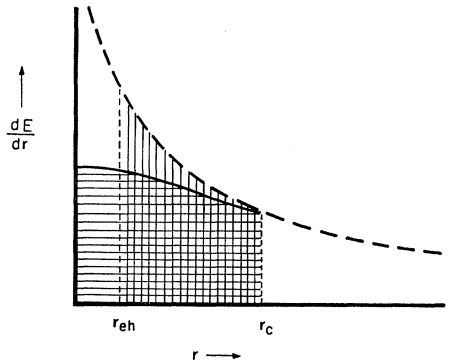

FIG. 4. Schematic plot of dE/dr as a function of r for a dislocation. r is the distance from the center of the dislocation, and E is the energy within a radius r. r_c and r_{eh} are the core and equivalent hole radii, respectively. The areas of the horizontally and vertically shaded regions are both numerically equal to the core energy.

curve in Fig. 4, has a singularity at the origin. Suppose that the actual curve follows the solid line, which must, of course, join the dashed line at the point beyond which the elastic theory holds. It is clear that a determination of the position of the solid line would allow the dislocation energy to be calculated because the area of the horizontally shaded region is equal to $E_{\text{core}}{}^{E}$, and the solid line joins the dashed line at $r_C{}^{E}$. All quantities in Eq. (5) would thus be determined.

It may be noted that Eq. (6) may be rewritten by using the substitution

$$E_{\text{core}}{}^{E}=\frac{\mu b^2}{4\pi(1-\nu)}\left(\ln\frac{r_C{}^{E}}{r_{\text{eh}}{}^{E}}\right), \tag{8}$$

where $r_{\text{eh}}{}^{E}$ is called the *equivalent hole radius* for the edge dislocation. (The meaning of this term will become apparent later.) Equation (6) then becomes

$$E^{E}(r)=\frac{\mu b^2}{4\pi(1-\nu)}\ln\frac{r}{r_{\text{eh}}{}^{E}}, \tag{9}$$

and this equation indicates that the dislocation behaves as if it obeyed linear elastic theory down to a radius $r_{\text{eh}}{}^{E}$, with the region inside this radius hollow. The position of $r_{\text{eh}}{}^{E}$ is clearly such that the area lying under the dashed curve between $r_{\text{eh}}{}^{E}$ and $r_C{}^{E}$ in Fig. 4 (the vertically shaded region) is equal to the area under the solid curve between $r=0$ and $r_C{}^{E}$ (the horizontally shaded region).[31]

B. Method of Computation

The edge dislocation examined in the present study lies along a ⟨112⟩ direction (in a {111} plane). Its Burgers vector was of the type $(a_0/2)\langle 110\rangle$. There are six different resolved atomic positions on a {112} plane normal to the dislocation line. These resolved positions are related to atoms in six successive different {112} planes. Outside of this set of planes the crystal is repeated. All relaxing operations need be carried out, therefore, only on atoms in these planes; and the crystal is made infinite along the dislocation line by the use of periodic boundary conditions which permit simultaneous movement of equivalent atoms. Calculations of the energy and atomic configuration of the dislocation were made for both elastic and atomistic models. In the first case the atoms were considered to be embedded in an elastic medium, and their displacements were then given by the isotropic elastic continuum theory. Their energies were calculated on the basis of interactions involving the Morse potential discussed elsewhere in this paper. This model will be designated *elasto-atomic*. It provided a convenient starting point for the atomistic calculation. In this second model the atoms were first located at the elasto-atomic positions and then allowed to relax until equilibrium prevailed.

The construction of the elasto-atomic dislocation involved some complications. Equations (4) are derived from a model in which the extra half-plane (having a thickness b, where b is the Burgers vector) is made by inserting an extra half-plane of thickness $b/2$ above the slip plane and removing a similar half-plane below the slip plane. Atomistic planes with thickness $b/2$ do not exist in the face-centered cubic lattice. The actual deformation of the perfect lattice corresponding to Eqs. (4) is shown in Fig. 5. It can be seen that the dislocation does not have the desired symmetrical form near the center. This difficulty was overcome by the process indicated in Fig. 6. The plane of the figure is {112}, and in this projection the 110 layers are stacked in an $ABABAB$ sequence in the perfect crystal [Fig. 6(a)]. The dotted line indicates the slip plane. Two adjacent A and B layers were effectively removed from the crystal by pushing the lower left quadrant of the crystal to

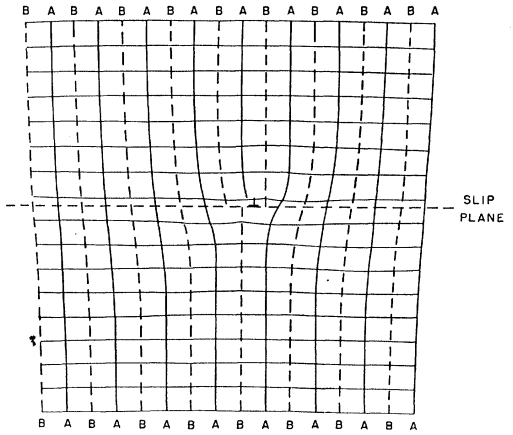

FIG. 5. A plot of the actual displaced positions of the atomic layers around an edge dislocation, as calculated from the linear isotropic elastic-continuum equations [Eqs. (4)]. Note that the planes of zero distortion parallel to the slip plane are offset.

[31] In reality the solid line in Fig. 4 is not continuous because the crystal is atomistic. The horizontally shaded region should therefore be replaced by a histogram having the same area.

the left by an amount b [Fig. 6(b)]. The B layer immediately to the right of the resulting gap was then moved to the left by an amount $b/2$ so as to bring it immediately below the A layer located on the origin [Fig. 6(c)]. The disturbed crystal was now symmetrical about the plane passing through the dislocation line. All atoms were then given the elastic displacements indicated by Eqs. (4).

As was noted previously, there are six different types of resolved atomic positions on a {112} plane in the fcc lattice. These arise from six consecutive different types of {112} planes. Outside these six planes the pattern is repeated. This fact permits considerable simplification of the computer calculations, because every atom outside these six basic planes is related to an atom in one of the six planes by a simple translation vector in the ⟨112⟩ direction. The crystal which is fed into the computer can therefore be made effectively infinite along the dislocation line by use of periodic boundary conditions. In the present study the number of atoms in each {112} plane was about 700.

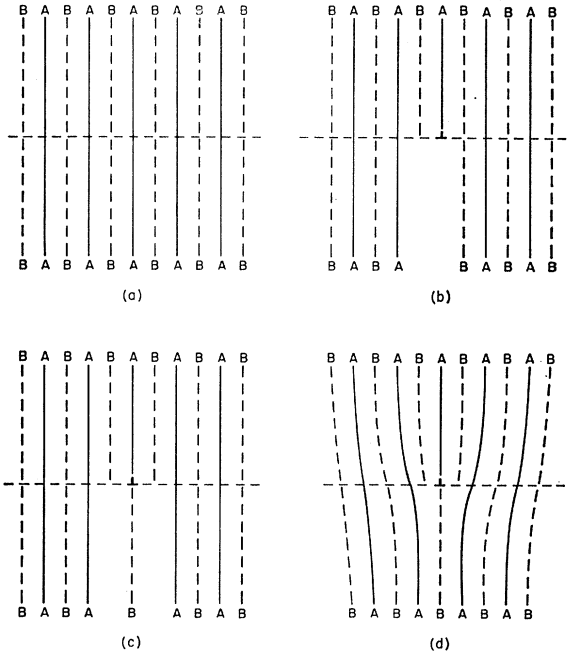

FIG. 6. Step-by-step procedure for the construction of the elasto-atomic edge dislocation by a method which overcomes the difficulties apparent in Fig. 5. A full description of the procedure is given in the text.

For convenience, the x and y axes were taken to lie in the (111) slip plane. They were placed along the $[1\bar{1}0]$ and $[11\bar{2}]$ directions, respectively. In order to facilitate the computer calculations, the units along these axes were chosen in such a way that the position of every atom in the perfect crystal could be given by integer coordinates. The units along the x, y, and z axes were $d/2$, $d/2\sqrt{3}$, and $(\sqrt{\frac{2}{3}})d$, respectively, where d is the nearest-neighbor distance. The dislocation was parallel to the y axis and cut the xz plane at $x=0$, $z=0.5$.

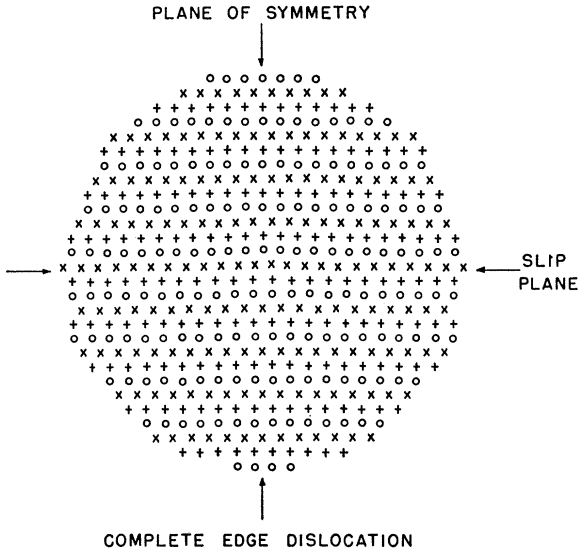

FIG. 7. Positions of atoms in three consecutive {112} planes normal to the complete edge dislocation line. It may be noted that the distortion of the lattice in the core region is not very severe. The core is neither hollow nor like a liquid.

The positions of the atoms in the perfect crystal were first fed into the computer; and the energy of each atom was calculated, the pairwise interactions being represented by the Morse potential function discussed earlier. The crystal was then deformed in such a way that the atoms were displaced to the elasto-atomic positions. The energy of the resulting elasto-atomic edge dislocation was calculated as a function of radial distance from the center of the dislocation. The atoms were then allowed

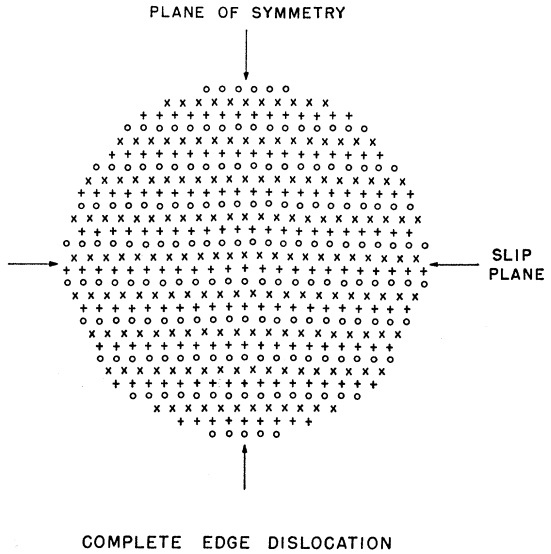

FIG. 8. Positions of atoms in three consecutive {112} planes immediately adjacent to the planes shown in Fig. 7.

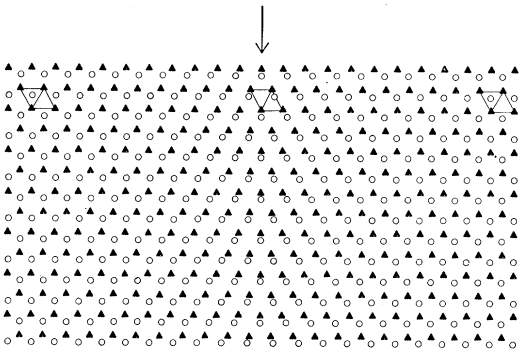

COMPLETE EDGE DISLOCATION

FIG. 9. Positions of atoms in two {111} planes, one above (triangles) and one below (circles) the slip plane of the complete edge dislocation. The dislocation line lies along the ⟨112⟩ direction indicated by the arrow.

to relax, one at a time, in a series of cycles, until equilibrium prevailed throughout the crystal.[32–34] The energy of the resulting atomistic dislocation was also calculated as a function of radial distance from the center of the dislocation. The strain energy inside a certain radius is $\frac{1}{2}\sum_{i=1}^{n}(E_i-E_0)$, where n is the number of atoms inside that radius, E_i is the energy of the ith atom after relaxation, and E_0 is the energy of an atom in the perfect crystal with respect to its 176 surrounding neighbors (see Sec. II). The factor $\frac{1}{2}$ allows for the fact that each bond between atoms is counted twice in the calculation. $E_0=7.07066$ eV.

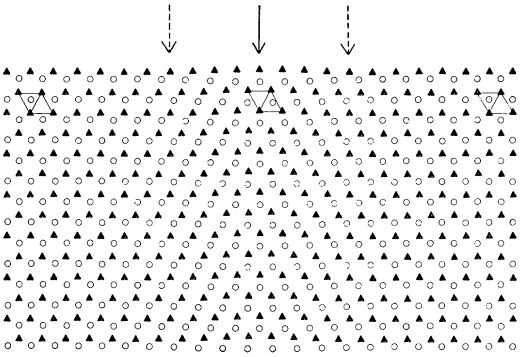

DISSOCIATED EDGE DISLOCATION

FIG. 10. Positions of atoms in two {111} planes, one above (triangles) and one below (circles) the slip plane of the dissociated edge dislocation. The position of the original complete dislocation line is along the ⟨112⟩ direction indicated by the full arrow. The partial dislocations, indicated by the dashed arrows, and the region of stacking fault which separates them can easily be distinguished by observing the figure from either side at a low angle.

C. Complete Edge Dislocation—Results

During the calculations for the complete dislocation the atoms were not permitted to relax in a direction parallel to the dislocation line. This prevented dissociation, as is discussed later. The positions of the atoms near the center of the dislocation are plotted in Figs. 7 and 8. As was noted in Sec. IVB, there are six nonequivalent {112} planes which lie normal to the dislocation line. The figure is therefore given in two parts for the sake of clarity, three planes being plotted on each half. It can be seen from the figure that the {111} planes parallel to the slip plane and close to it show appreciable distortion. Figures 9 and 10 are views looking down onto the slip plane. They show the positions of atoms in the {111} plane immediately below the slip plane and the {111} plane immediately above the slip plane. The positions of some of the atoms close to the center of the dislocation are given in Tables II and III. Also given in the tables are the energy of each atom, E_i, and its distance from the center of the dislocation.

The energy of the complete dislocation is plotted as a function of radius in Fig. 11. Both the elasto-atomic and atomistic energies are given. The energies have been plotted against $\ln r$ so that the extent of the linear region of the curve [which would be in agreement with Eq. (9)] can clearly be seen.

V. CALCULATION OF THE ENERGY AND ATOMIC CONFIGURATION OF A DISSOCIATED EDGE DISLOCATION—RESULTS

The final positions attained by the atoms in the study of the complete edge dislocation were used as the initial positions in the examination of the dissociated dislocation. When the atoms were allowed to relax in a direction parallel to the dislocation, the dislocation spontaneously dissociated. The positions of the atoms near the dissociated dislocation are shown in Fig. 10 (which is to be compared with Fig. 9). Two distinct partial dislocations can be observed in Fig. 10, and the region between them contains a stacking fault. The separation distance between the partials is approximately 20 Å or 8b. There are at least two reasons why this separation distance might be in error. They are discussed in Sec. VI of this paper.

The energy of the dissociated dislocation is plotted as a function of radius in Fig. 11. This curve has been made to correspond as closely as possible with that of the complete dislocation. The radius in Fig. 11 is measured from the center of the original complete dislocation.

[32] This process, and also the question of corrections for the double counting of atomic bonds, is discussed in greater detail elsewhere (Refs. 33, 34).

[33] M. Doyama and R. M. J. Cotterill, Phys. Rev. **137**, A994 (1965).

[34] R. M. J. Cotterill and M. Doyama, *Lattice Defects in Quenched Metals*, edited by R. M. J. Cotterill, M. Doyama, J. J. Jackson, and M. Meshii (Academic Press Inc., New York, 1965), p. 653.

TABLE II. Positions and energies of atoms around elasto-atomic edge dislocation.

Identity			Coordinates x	y	z	Distance from the center	Energy E_i (eV)
1	3	0	0.000	3.000	0.046	0.371	−7.449
0	4	1	0.000	4.000	1.046	0.446	−5.509
−1	1	1	−0.929	1.000	0.903	0.569	−5.816
1	1	1	0.929	1.000	0.903	0.569	−5.816
2	0	0	1.243	0.000	−0.068	0.775	−6.878
−2	0	0	−1.243	0.000	−0.068	0.775	−6.878
−2	4	1	−1.757	4.000	0.856	0.925	−6.162
2	4	1	1.757	4.000	0.856	0.925	−6.162
0	2	2	0.000	2.000	1.990	1.216	−7.070
1	5	−1	0.000	5.000	−1.010	1.233	−7.269
3	3	0	2.330	3.000	−0.127	1.273	−6.921
−3	3	0	−2.330	3.000	−0.127	1.273	−6.921
−1	5	2	−0.982	5.000	1.966	1.294	−6.940
1	5	2	0.982	5.000	1.966	1.294	−6.940
−3	1	1	−2.670	1.000	0.838	1.363	−6.373
3	1	1	2.670	1.000	0.838	1.363	−6.373
2	2	−1	1.071	2.000	−1.039	1.366	−7.175
−2	2	−1	−1.071	2.000	−1.039	1.366	−7.175
−2	2	2	−1.929	2.000	1.917	1.506	−7.080
2	2	2	1.929	2.000	1.917	1.506	−7.080
3	5	−1	2.136	5.000	−1.082	1.676	−7.000
−3	5	−1	−2.136	5.000	−1.082	1.676	−7.000
4	0	0	3.375	0.000	−0.157	1.771	−7.016
−4	0	0	−3.375	0.000	−0.157	1.771	−7.016
−3	5	2	−2.864	5.000	1.875	1.820	−7.026
3	5	2	2.864	5.000	1.875	1.820	−7.026
−4	4	1	−3.625	4.000	0.824	1.832	−6.865
4	4	1	3.625	4.000	0.824	1.832	−6.865
0	0	3	0.000	0.000	2.963	2.011	−7.042
−1	3	3	−0.989	3.000	2.955	2.064	−7.034
1	3	3	0.989	3.000	2.955	2.064	−7.034
1	1	−2	0.000	1.000	−2.037	2.071	−7.057
4	2	−1	3.196	2.000	−1.119	2.074	−6.998
−4	2	−1	−3.196	2.000	−1.119	2.074	−6.998
2	4	−2	1.036	4.000	−2.048	2.144	−7.046
−2	4	−2	−1.036	4.000	−2.048	2.144	−7.046
−4	2	2	−3.804	2.000	1.847	2.197	−6.985
4	2	2	3.804	2.000	1.847	2.197	−6.985
−2	0	3	−1.964	0.000	2.931	2.214	−7.035
2	0	3	1.964	0.000	2.931	2.214	−7.035
5	3	0	4.402	3.000	−0.175	2.269	−7.042
−5	3	0	−4.402	3.000	−0.175	2.269	−7.042
−5	1	1	−4.598	1.000	0.812	2.313	−6.998
5	1	1	4.598	1.000	0.812	2.313	−6.998
3	1	−2	2.071	1.000	−2.072	2.341	−7.036
−3	1	−2	−2.071	1.000	−2.072	2.341	−7.036
−3	3	3	−2.929	3.000	2.901	2.447	−7.059
3	3	3	2.929	3.000	2.901	2.447	−7.059
5	5	−1	4.243	5.000	−1.147	2.512	−7.021
−5	5	−1	−4.243	5.000	−1.147	2.512	−7.021
−5	5	2	−4.757	5.000	1.828	2.614	−6.995
5	5	2	4.757	5.000	1.828	2.614	−6.995
4	4	−2	3.110	4.000	−2.099	2.631	−7.040
−4	4	−2	−3.110	4.000	−2.099	2.631	−7.040

TABLE III. Positions and energies of atoms around complete edge dislocation.

Identity			Coordinates x	y	z	Distance from the center	Energy E_i (eV)
1	3	0	−0.002	3.000	−0.078	0.472	−7.325
0	4	1	0.001	4.000	0.984	0.395	−6.265
−1	1	1	−0.914	1.000	0.968	0.596	−6.337
1	1	1	0.916	1.000	0.968	0.597	−6.335
2	0	0	1.104	0.000	−0.090	0.732	−7.279
−2	0	0	−1.107	0.000	−0.090	0.734	−7.278
−2	4	1	−1.836	4.000	0.935	0.984	−6.488
2	4	1	1.838	4.000	0.935	0.986	−6.483
0	2	2	0.000	2.000	1.982	1.210	−6.896
1	5	−1	−0.001	5.000	−1.071	1.283	−7.032
3	3	0	2.200	3.000	−0.113	1.209	−7.207
−3	3	0	−2.202	3.000	−0.113	1.210	−7.205
−1	5	2	−0.960	5.000	1.972	1.294	−6.914
1	5	2	0.961	5.000	1.972	1.294	−6.913
−3	1	1	−2.769	1.000	0.904	1.423	−6.631
3	1	1	2.771	1.000	0.904	1.424	−6.628
2	2	−1	1.056	2.000	−1.077	1.392	−7.031
−2	2	−1	−1.057	2.000	−1.078	1.392	−7.031
−2	2	2	−1.917	2.000	1.946	1.521	−6.952
2	2	2	1.918	2.000	1.947	1.522	−6.951
3	5	−1	2.112	5.000	−1.096	1.677	−7.026
−3	5	−1	−2.113	5.000	−1.096	1.678	−7.026
4	0	0	3.268	0.000	−0.135	1.714	−7.163
−4	0	0	−3.270	0.000	−0.135	1.715	−7.162
−3	5	2	−2.874	5.000	1.917	1.845	−6.981
3	5	2	2.875	5.000	1.917	1.845	−6.980
−4	4	1	−3.715	4.000	0.877	1.883	−6.752
4	4	1	3.716	4.000	0.877	1.883	−6.749
0	0	3	0.000	0.000	2.966	2.013	−7.020
−1	3	3	−0.974	3.000	−2.959	2.066	−7.024
1	3	3	0.975	3.000	2.959	2.066	−7.024
1	1	−2	0.000	1.000	−2.073	2.101	−7.040
4	2	−1	3.164	2.000	−1.118	2.061	−7.024
−4	2	−1	−3.166	2.000	−1.118	2.062	−7.024
2	4	−2	1.035	4.000	−2.078	2.167	−7.037
−2	4	−2	−1.036	4.000	−2.078	2.168	−7.038
−4	2	2	−3.835	2.000	1.890	2.227	−6.996
4	2	2	3.834	2.000	1.890	2.228	−6.995
−2	0	3	−1.947	0.000	2.943	2.219	−7.034
2	0	3	1.948	0.000	2.943	2.219	−7.034
5	3	0	4.320	3.000	−0.154	2.225	−7.138
−5	3	0	−4.322	3.000	−0.154	2.226	−7.139
−5	1	1	−4.671	1.000	0.854	2.353	−6.848
5	1	1	4.672	1.000	0.854	2.354	−6.846
3	1	−2	2.071	1.000	−2.090	2.355	−7.039
−3	1	−2	−2.072	1.000	−2.091	2.355	−7.040
−3	3	3	−2.916	3.000	2.919	2.455	−7.047
3	3	3	2.917	3.000	2.920	2.456	−7.047
5	5	−1	4.209	5.000	−1.139	2.494	−7.029
−5	5	−1	−4.210	5.000	−1.139	2.494	−7.030
−5	5	2	−4.795	5.000	1.866	2.644	−7.005
5	5	2	4.796	5.000	1.866	2.645	−7.004
4	4	−2	3.108	4.000	−2.108	2.636	−7.039
−4	4	−2	−3.108	4.000	−2.108	2.636	−7.039

This means that in most cases points in the two figures correspond to the same atoms. Clearly, the energy of dissociation is the vertical distance between the asymptotic regions of the two curves. It must be emphasized again, however, that this will only be the true dissociation energy if the separation distance of the partials is the true separation distance. As was noted earlier, and as will be discussed in Sec. VI, it is quite unlikely that the true separation distance is obtained in the present calculations. The positions of the atoms surrounding the dissociated edge dislocation are given in Table IV.

TABLE IV. Positions and energies of atoms around dissociated edge dislocation.

Identity			Coordinates x	y	z	Distance from the center	Energy E_i (eV)
1	3	0	−0.001	2.580	−0.115	0.502	−7.184
0	4	1	−0.001	4.393	0.885	0.315	−6.816
−1	1	1	−0.957	1.379	0.887	0.573	−6.798
1	1	1	0.955	1.379	0.887	0.573	−6.801
2	0	0	1.052	−0.416	−0.115	0.727	−7.191
−2	0	0	−1.053	−0.416	−0.115	0.727	−7.191
−2	4	1	−1.911	4.332	0.891	1.007	−6.755
2	4	1	1.910	4.333	0.891	1.007	−6.757
0	2	2	0.000	2.219	1.901	1.144	−7.021
1	5	−1	0.000	4.802	−1.099	1.306	−7.060
3	3	0	2.106	2.601	−0.114	1.167	−7.208
−3	3	0	−2.108	2.602	−0.114	1.167	−7.208
−1	5	2	−0.966	5.215	1.902	1.242	−7.019
1	5	2	0.965	5.213	1.902	1.242	−7.021
−3	1	1	−2.860	1.260	0.895	1.466	−6.702
3	1	1	2.860	1.262	0.895	1.466	−6.705
2	2	−1	1.049	1.803	−1.099	1.407	−7.063
−2	2	−1	−1.050	1.803	−1.099	1.408	−7.064
−2	2	2	−1.931	2.196	1.904	1.499	−7.012
2	2	2	1.931	2.195	1.904	1.498	−7.014
3	5	−1	2.097	4.811	−1.101	1.676	−7.068
−3	5	−1	−2.099	4.811	−1.101	1.676	−7.070
4	0	0	3.160	−0.369	−0.118	1.658	−7.231
−4	0	0	−3.161	−0.368	−0.117	1.659	−7.232
−3	5	2	−2.898	5.166	1.905	1.848	−6.998
3	5	2	2.897	5.165	1.905	1.848	−7.000
−4	4	1	−3.806	4.175	0.893	1.930	−6.677
4	4	1	3.807	4.177	0.893	1.930	−6.678
0	0	3	0.000	0.125	2.908	1.966	−7.058
−1	3	3	−0.972	3.124	2.908	2.025	−7.057
1	3	3	0.973	3.123	2.908	2.026	−7.057
1	1	−2	0.000	0.927	−2.090	2.115	−7.047
4	2	−1	3.142	1.825	−1.107	2.047	−7.070
−4	2	−1	−3.143	1.825	−1.107	2.047	−7.069
2	4	−2	1.038	3.925	−2.091	2.179	−7.050
−2	4	−2	−1.039	3.926	−2.091	2.178	−7.050
−4	2	2	−3.865	2.129	1.901	2.246	−6.989
4	2	2	3.864	2.128	1.901	2.245	−6.986
−2	0	3	−1.946	0.115	2.908	2.194	−7.054
2	0	3	1.946	0.114	2.908	2.194	−7.053
5	3	0	4.213	2.673	−0.127	2.168	−7.240
−5	3	0	−4.215	2.675	−0.127	2.169	−7.240
−5	1	1	−4.753	1.092	0.884	2.397	−6.700
5	1	1	4.752	1.093	0.884	2.397	−6.698
3	1	−2	2.076	0.927	−2.095	2.359	−7.050
−3	1	−2	−2.077	0.927	−2.095	2.359	−7.049
−3	3	3	−2.920	3.099	2.906	2.448	−7.050
3	3	3	2.920	3.101	2.905	2.447	−7.049
5	5	−1	4.183	4.847	−1.117	2.474	−7.070
−5	5	−1	−4.184	4.846	−1.117	2.474	−7.070
−5	5	2	−4.832	5.093	1.891	2.670	−6.986

VI. DISCUSSION

It can be seen from Figs. 7, 8 and 9 that the complete edge dislocation is not very wide. Formally, the width is defined as being the range of x within which the displacement is less than one-half of its limiting value (i.e., $-b/8 \leqslant u(x) \leqslant b/8$).[35,36] Using this criterion, the dislocation in the present study is found to have a width of 5b.

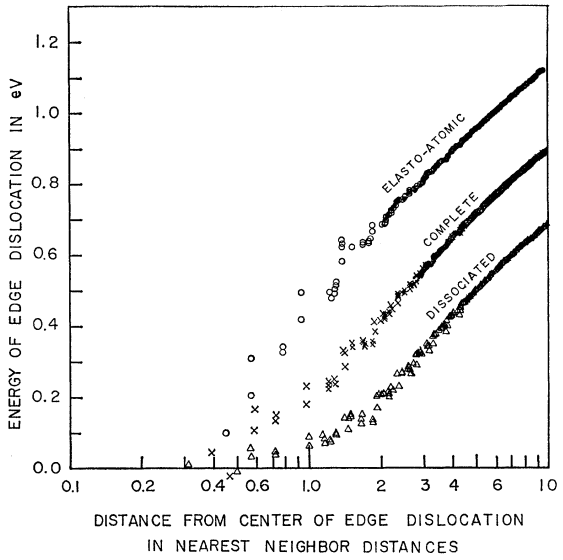

FIG. 11. Energy within a given radius as a function of that radius as measured from the center of an edge dislocation. The three cases, elasto-atomic, complete, and dissociated, are shown. The energy given in the figure is for a length $d_0/2\sqrt{3}$ of dislocation.

It may be noted here that the distortion of the lattice in the core region is not very severe. The core is certainly not hollow; neither could it be said to be a good approximation to a liquid.

The energy plot of Fig. 11 is, of course, directly related to Fig. 4. The point at which the atomistic curve deviates from a straight line is equivalent to the point at which the solid and dashed lines meet in Fig. 4 (i.e., the point at which $r=r_C{}^E$). Thus the core radius can be read off directly from Fig. 11 and one obtains a value

$$r_C{}^E = 3.6 d_0. \tag{10}$$

Furthermore, the energy at that point is equivalent to the horizontally shaded region of Fig. 4 and is simply the core energy. In the present case this is

$$E_{\text{core}}{}^E = 0.65 \text{ eV per } d_0/2\sqrt{3}. \tag{11}$$

This value is generally about twice as large as the previous estimates listed in the Introduction. It might be noted here, however, that all calculations using a Morse potential based on the experimental value of E_S give defect energies which are too high by a factor of about 3.[20,24] If that correction is made here, the calculated core energy is slightly below previous estimates.

Finally, it will be noted that the intercept on the $\ln r$ axis of the extrapolated straight-line region in Fig. 11

[35] A. H. Cottrell, *Dislocations and Plastic Flow in Crystals* (Clarendon Press, Oxford, England, 1953), p. 61.
[36] A. J. Foreman, M. A. Jaswon, and J. K. Wood, Proc. Phys. Soc. (London) **A64**, 156 (1951).

is equal to $r_{eh}{}^{E}$, the equivalent hole radius in Fig. 4. This is found to be

$$r_{eh}{}^{E}=0.3d_0. \tag{12}$$

A calculation of the dislocation energy using the elastic continuum Eq. (9) and this value of $r_{eh}{}^{E}$ would automatically take into account the true energy of the core.

A remark about terminology may be appropriate here. It will be noted that the term *cutoff radius* has not been used. This is to avoid ambiguity because that term might reasonably be applied to both $r_C{}^{E}$ and $r_{eh}{}^{E}$. On the other hand, the terms *core radius* and *equivalent hole radius* are quite apposite in that they can be applied to these two radii respectively without risk of confusion.

The spontaneous dissociation of the edge dislocation, when the atoms are allowed to move in the y direction, is clearly demonstrated by the difference between Fig. 9 and Fig. 10. The equilibrium separation distance of the partial dislocations is achieved when the repulsive force between them is just balanced by the attractive force of the stacking fault which separates them. If conditions were such that no other factors affected the separation, one could, in principle, make an estimate of the stacking-fault energy using this distance.

The magnitude of the force per unit length between two parallel infinite complete pure edge dislocations is[37]

$$F^{E}=\frac{\mu b_1{}^{E}b_2{}^{E}}{2\pi(1-\nu)r}, \tag{13}$$

where b_1 and b_2 are the Burgers vectors of the respective dislocations, and r is the distance of separation. The corresponding force between screw dislocations is

$$F^{S}=\frac{\mu b_1{}^{S}b_2{}^{S}}{2\pi r}. \tag{14}$$

For a dissociated edge dislocation the partials have both edge and screw components, where $b_1{}^{E}=d_0/2$, $b_2{}^{E}=d_0/2$, $b_1{}^{S}=d_0/2\sqrt{3}$, and $b_2{}^{S}=-d_0/2\sqrt{3}$. The force per unit length between the partials, when they are separated by a distance r, is

$$F=F^{E}+F^{S}=\frac{\mu d_0{}^{2}}{8\pi(1-\nu)r}-\frac{\mu d_0{}^{2}}{24\pi r}. \tag{15}$$

The force per unit length due to the stacking fault is simply $-\gamma$. Thus the total force trying to separate the partials is

$$F^{\text{total}}=\frac{\mu d_0{}^{2}}{8\pi r}\left\{\frac{1}{(1-\nu)}-\frac{1}{3}\right\}-\gamma. \tag{16}$$

Equating F^{total} to zero, we obtain the equilibrium separation of the partials, $r_{eq}{}^{E}$.

$$r_{eq}{}^{E}=\frac{\mu d_0{}^{2}}{24\pi r}\left\{\frac{2+\nu}{1-\nu}\right\}. \tag{17}$$

Using the experimental values for copper, $\mu=4.9\times10^{11}$ dyn cm^{-2}, $d_0=2.5$ Å, $\gamma\simeq60$ erg cm^{-2} [26–28] and $\nu=0.3$, we obtain

$$e_{eq}{}^{E}\simeq18\text{Å}. \tag{18}$$

In the present calculations, however, there are at least two reasons why the separation distance might be in error. It must be noted that the present calculations are strictly applicable only to the absolute zero temperature so that the two partials have no chance of overcoming the Peierls-Nabarro barrier.[38,39] The situation is shown

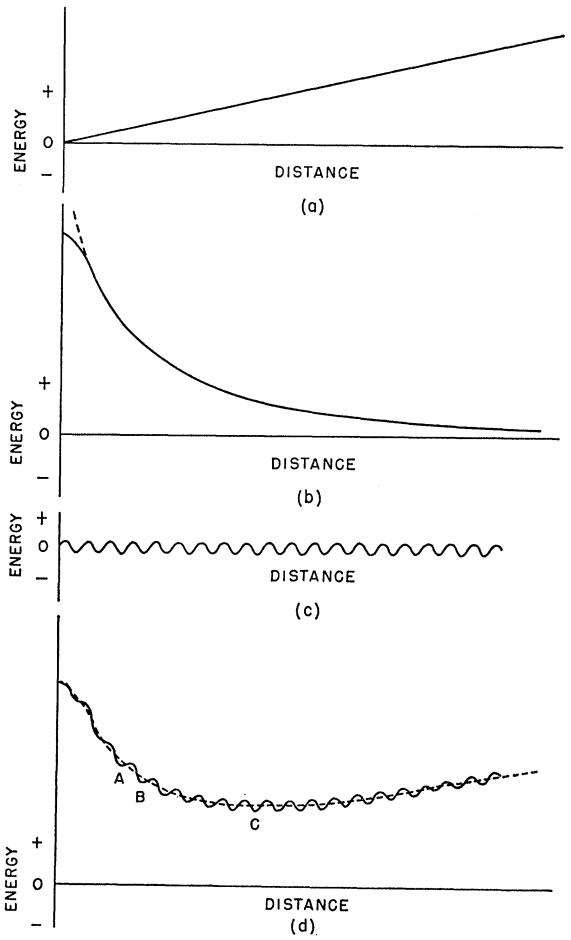

FIG. 12. Schematic plot of the relative energies of a system of two partial dislocations separated by a stacking fault. The relative energies are shown as a function of the distance separating the partials. The first three curves show the separate components arising from (a) the stacking fault, (b) the interaction between the partials, and (c) Peierls-Nabarro barrier. Curve (d) is the result of summing the various components.

[37] A. H. Cottrell, Ref. 35, p. 45.

[38] R. Peierls, Proc. Phys. Soc. (London) **52**, 34 (1940).

[39] F. R. N. Nabarro, Proc. Phys. Soc. (London) **59**, 256 (1947).

in Fig. 12, and there are three energy components to be considered. The stacking-fault term increases linearly with separation, while the interaction term falls asymptotically to zero. The Peierls-Nabarro energy is periodic (but, of course, is not necessarily sinusoidal). Summing up these three contributions, we obtain the net energy curve shown at the bottom of the figure. It can be seen from the figure that even at the absolute zero temperature, the complete dislocation will move to position A. This position is probably the one which is achieved by the second partial dislocation in the present calculations. At a finite temperature the partial could move to position B, and eventually by a series of jumps to C, by a thermally activated process. The second source of error concerns the stacking-fault term itself. If the stacking fault which appears between the partials is to play its proper role in determining the separation distance, the stacking-fault energy predicted by the model would have to match the true value of that parameter. This poses considerable difficulty. Details of a calculation of the stacking-fault energy of copper based on the Morse potential are given in Sec. III. It is found that the calculated stacking-fault energy depends upon the truncation of the potential. For no truncation the value is close to 1 erg cm^{-2}. This is only about 2% of the experimental value for copper. Truncation at 176 neighbors gives an "artificial" value of 30 erg cm^{-2}. This is the main reason why this truncation was used in the calculations.

SUMMARY

The calculations described here demonstrate the fact that a three-dimensional atomistic crystal with central forces is capable of supporting a dislocation which has all the features expected of such a defect in a real crystal. The dissociation of a complete dislocation, which on the basis of experiment is known to occur in practice, is observed in the model; and within the framework of the calculations reliable energies and atomic configurations are obtained. With certain precautions this method might even give meaningful values of stacking-fault energy. Because theoretical work on dislocations is now inclining towards investigations of their interactions with point defects, which are themselves best treated through atomistic models, it is believed that the approach adopted here is superior to methods which employ the elastic-continuum theory.

The specific dislocation examined here was the edge dislocation in copper. A variational method was employed (with the aid of a digital computer), and the pairwise interaction between discrete atoms was represented by a Morse potential function. For the complete dislocation it was necessary to impose a constraint which prevented atoms from relaxing in a direction parallel to the dislocation line. This prevented dissociation. For the complete dislocation [Burgers vector $(a_0/2)\langle 110\rangle$] linear elastic theory was found to break down inside a *core radius* of 9 Å. The corresponding core energy, 0.65 eV per {112} plane, is somewhat greater than most previous estimates, but it is shown that the calculated value may be too high by a factor of about 3. If the core is replaced by a cylindrical hole of radius r_{eh} (the *equivalent hole radius*), the inside of which is hollow and outside of which linear elastic theory holds at all points, this radius is 0.8 Å. The complete dislocation was found to have a width of 13 Å (i.e., 5b). The core was found to be neither hollow nor like a liquid.

The removal of the constraint on the atomic relaxations permitted spontaneous dissociation of the dislocation into two Heidenreich-Shockley partials. This process involves no activation energy.

For the Morse potential a stacking fault of infinite extent in copper has an energy of 30 erg cm^{-2} (for a truncation at 176 neighboring atoms). It was found that certain precautions must be taken to ensure that the separation distance of the partial dislocations is the same as the distance given by elastic theory. A whole series of interatomic potentials was used in the calculations of stacking-fault energy, and the derived values of this parameter were found to be critically dependent upon the potential used. A preliminary account of this type of calculation has been published previously.[40,41]

ACKNOWLEDGMENTS

It is a pleasure to acknowledge the interest and encouragement of T. H. Blewitt, H. H. Chiswik, F. G. Foote, and O. C. Simpson. The computer calculations were greatly facilitated by the cooperation and diligence of C. LeVee and the scheduling, consulting, and operating personnel of the Argonne CDC 3600 computer.

---

[40] M. Doyama and R. M. J. Cotterill, Phys. Letters **13**, 110 (1964).

[41] R. M. J. Cotterill and M. Doyama, Phys. Letters **14**, 79 (1965).